Volume 9, Issue 2, 092507 (1-7)

Signal Processing and Renewable Energy (SPRE)

https://doi.org/10.57647/j.spre.2025.0902.07

Non-blind image restoration using hidden markov modeling and minimum entropy approach

Leila Ghabeli[1,*], Hamidreza Amindavar[2]

[1]*Department of Electrical Engineering, Islamic Azad University, CT.C. (Central Tehran Branch), Tehran, Iran.*
[2]*Department of Electrical Engineering, Amirkabir University of Technology, Tehran, Iran.*

[*]**Corresponding author:** lghabeli@iau.ac.ir

Original Research

Received:
9 January 2025
Revised:
22 January 2025
Accepted:
26 April 2025
Published online:
1 June 2025

Abstract:

In this paper, a new method based on HMM (Hidden Markov Models) is presented for image restoration. We assume that the image is treated by a finite impulse response (FIR) blur or channel where the image is modeled as a Markov process. The superior property of this new method is the detection of the most likely gray level for each pixel based on the probabilities defined for both the noisy blurred observations and the original image. We also propose a new method to find the more structured region of the image based on the minimum entropy approach. The performance of the proposed algorithm is illustrated through simulations employing blurred images with different point spread functions. Comparison between the introduced method and the other proposed methods shows the superiority of the HMM method especially for large spreading blurs.

Keywords: Hidden markov models; Finite impulse response; Non-blind; Image restoration; Minimum entropy

1. Introduction

Blind image restoration is a common yet challenging problem. In pattern recognition problems, the effectiveness of the analysis depends heavily on the quality of the image to be processed. This image may be blurred and noisy. As another example, turbulence decreases the imaging effect of remote sensing imaging equipment in various scenes, as the distortion caused by turbulence includes changes in spatial blur, geometric distortion, and interference due to sensor noise. The goal of digital image restoration is to reconstruct the original scene from a degraded observation. A fundamental issue in this process is blur estimation, when the blur is not readily available, it has to be estimated from the observed image.

Except for some early works [1–7], little work has been done for nonblind image restoration i.e., where the blur is known or is estimated by some preprocessing methods. Two main approaches have been proposed for this purpose. The first one identifies the blur parameters before any restoration [1] whereas the second one realizes these two steps jointly [2].

Among the proposed methods for deconvolution, the regularized filter introduced by Tikhonov [3] has been well known. In many proposed methods for blind image restoration [1], after determining the channel taps, a regularized filter is used for the deconvolution process. In [8], a corrupted image that has been affected by various noise and motion blur has been considered. A recovery model has been presented, followed by an algorithm based on the radial basis function network (RBFN). Additionally, a method based on object extraction is proposed for recovering a locally blurred image to address the problem of poor recovery results when the overall motion blur features are lost for locally blurred images.

In the last decade, a huge number of works for image restoration have been done by taking advantage of supervised, semi-supervised, unsupervised, and deep learning [9–11]. Classical and deep learning methods represent different approaches to this problem, each with its advantages and disadvantages. Also, the degradation of quality in the real world is more complex than that of synthetic datasets. Significant progress has been made with the supervised models on paired synthetic data.

In [9] an unsupervised deblurring framework based on self-

augmentation has been proposed. This framework gradually generates improved pseudo-clear and blurry image pairs without the need for real paired datasets, and the generated image pairs with higher qualities can be used to enhance the performance of the restorer.

In [10], a solution based on the integration of mathematical interpolation and deep learning has been proposed to reduce distortion and blur. In the first stage, a thin plate spline is used to reduce the turbulence imaging distortion. In the second stage, a convolutional neural network containing a lightweight residual feature extraction module is used to address blur.

In [11], a blind image recovery method has been proposed and a variable inference algorithm has been designed, in which all expected posterior distributions are parameterized as deep neural networks to improve the model capabilities.

This paper switches to old methods to highlight and show their nice power and superiorities that surely can still be considered in accompany with the new methods of recent days to improve the results qualities. In this way, we propose a nonblind image restoration method which is useful under circumstances where the blur estimation and restoration processes are performed separately. The basic idea behind our method is similar to the algorithms proposed for channel equalization in the communication paradigm [4, 5]. The digital communications methods for channel equalization based on the finite state Markov process are appealing for image restoration because they solve the problem using the expectation maximization (EM) algorithm in the maximum likelihood sense.

Here we introduce some modifications to the algorithms of [4], and [5] in order to improve their performance and suitability for image restoration. This is done by defining two kinds of probabilities, the probability of the noisy observations and the probabilities of the gray level occurrences for local neighborhood pixels. The second probability is highly affected by the size of the window, whenever the selected region by a window is smoother, the estimation is more reliable. In this paper, we also propose a new algorithm based on the minimum entropy to detect the more structured region across the image. The window size around each pixel is estimated so that the acquired region has more structured data. As it is inferred from the experiments, the performance of the HMM method in conjunction with the minimum entropy approach to construct a suitable window is higher especially when the blur is too extended.

The paper is organized as follows: In section 2, the system model for the noisy blurred image is described. The new proposed method for image restoration is introduced in section 3. The simulation results are shown in section 4. Finally, in section 5 some concluding remarks are provided.

2. System model

We assume the original image is affected by a two-dimensional linear shift-invariant FIR filter, and observed in the presence of an additive noise. Hence, the corresponding degraded image $o(x,y)$ for a given ideal image $A(x,y)$, is modeled as:

$$o(i,j) = \sum_{|x|\leq \frac{X}{2}} \sum_{|y|\leq \frac{Y}{2}} h(x,y)A(i-x,j-y) + n(i,j) \qquad (1)$$

for any $1 \leq i \leq I$, $1 \leq j \leq J$, where I, J denote the horizontal and vertical sizes of image, respectively. $h(x,y)$ denotes the entries of $X \times Y$ matrix $\mathbb{H} \cdot \mathbb{H}$ stands for the impulse response of the linear shift-invariant FIR channel or blur, $(X \times Y)$ is usually known as the blur extend, and $n(i,j)$ denotes the additive noise which is assumed as a zero-mean white Gaussian process with variance S_n^2. In order to create the observation sequence, the image is scanned in the horizontal direction. We define the state matrix of the hidden Markov process as the matrix that contains all the pixels stored in the channel memory to produce the observation at pixel (i,j), i.e., the blurred pixels, thus the size of this matrix is equal to the size of the blur, i.e.$X \times Y$. By assuming N possible values, $\{q_1, q_2, \ldots, q_N\}$, for the gray levels of the image, the state matrix can be modeled as a first order Markov process with N^{XY} individual states $\{Q_1, Q_2, \ldots, Q_{N^{XY}}\}$, where Q_n for $1 \leq n \leq N^{XY}$ denotes the $X \times Y$ matrix with entries belongs to $\{q_1, q_2, \ldots, q_N\}$. Next, we describe the new image restoration algorithm based on HMM and minimum entropy strategy.

3. The proposed nonblind image restoration method

In this section, we introduce the proposed method of this paper for nonblind image restoration based on HMM and minimum entropy approaches.

In the first stage, we obtain an initial estimate of the original image with the aid of the well-known restoration method, the Wiener filter [6], then by using this initial restored image we provide the probabilities of gray levels, $\Pr\{q_n\}$, for the restoration process. Among the non-blind image restoration methods, the restored images by the Wiener filter have higher root mean square value than the other methods but it maintains the details of the image along with the noise effect, so repeating the Wiener filtering algorithm more than two steps doesn't improve the performance since the resolution of the autocorrelation of the observed image in (1) is the same as the second step, hence no benefit is extracted.

In the second stage, we propose a new method based on the minimum entropy approach to determine the size of the window for the image restoration algorithm. As we know the size of the region that is used for the estimation of the local mean and variance is also important in the restoration process. Since entropy provides a measure of the uncertainty about the information available in an image, the optimal choice of the window size should be related to this quantity.

In the third stage, the restored image acquired by the Wiener filter is used as the initial image, and the HMM algorithm is applied. Because a Wiener filtering approach implements the near-optimal minimum mean square estimation of the blurred image and the HMM method provides a further reduction in the variance of the estimated image due to EM maximum likelihood convergence property, it is expected that an enhanced image quality restoration is obtained by

combining the Wiener filter and EM in HMM. The experiments also verify that the restored image is of higher quality than the restored image of the first stage.
In the fourth stage, the restored image acquired by the HMM algorithm is used as the initial image, and the HMM algorithm is applied again to this initial image. The experiments verify that the restored image in the fourth stage is of higher quality than the restored image in the third step.

3.1 The proposed minimum entropy window size selection

The purpose of this algorithm is to detect the more structured region with minimum entropy in the neighborhood of each pixel. The minimum entropy region at each pixel is the region that has the minimum entropy value among the larger and all smaller regions at that pixel. This region expresses the more homogeneous and structured region that we can remove noise from with less concern about losing the details.
Let's assume a finite set of window sizes: $W = \{w_1, w_2, \ldots, w_L\}$ at pixel (i,j) starting with quite small window size w_1 and then determine a sequence of the entropy values $H_l(i,j)$, $(1 \le l \le L)$ associated with each of the window sizes, then adaptive window size is given by the following rule: consider the values $H_l(i,j)$, $1 \le l \le L$, with increasing L. The adaptive window size is the largest of those L windows for which the entropy values $H_l(i,j)$, $1 \le l \le L$, have the decreasing trend. Based on this rule the window size at each pixel is increased until the computed entropy value for it becomes larger than its previous value in the smaller window. This algorithm is justified based on the concept of the entropy that introduces the amount of randomness, thus the minimum entropy criterion achieves more structured regions. In the following, the definition of entropy is presented and by extending the entropy formulation it is shown how the entropy algorithm acquires the favorite window size. The entropy value for a window around pixel (i,j) with size w_1 is defined as,

$$H_l(i,j) = -\sum_{n=1}^{N} \Pr\{\hat{A}(i,j) = q_n\} \log(\Pr\{\hat{A}(i,j) = q_n\}), \tag{2}$$

where $\hat{A}$ denotes the estimated image obtained through previous steps, and $\Pr\{\hat{A}(i,j) = q_n\}$ in (2) denotes the probability that the original pixel value at (i,j) is equal q_n.
Since Gaussian processes are probably the simplest way of specifying a non-trivial prior probability distribution function overall probability function spaces, in our work we use the Gaussian distribution to model the probability density of the gray levels of the neighborhood pixels, according to the principle of insufficient reasoning due to Bernoulli for all the possibilities, i.e.; gray levels, follow the same probability distribution function given the mutually exclusive observations $o(i,j)$ and no further information. On the other hand, this assumption is justified based on the fact that the underlying distribution of the random variable whose mean and variance are fixed and maximize the entropy is Gaussian, hence, in the absence of the knowledge of the true gray level probability density functions, the worst possible scenario is assumed. Since under almost all possible circumstances, images have local stationary statistics and there are some spatial relationships among neighboring pixels in a window.
By assuming the Gaussian probability density for the local pixels, we have

$$\Pr\{\hat{A}(i,j) = q_n\} = N(m_{\hat{A}}(i,j); S^2_{\hat{A}}(i,j)), \tag{3}$$

where $m_{\hat{A}}(i,j)$ and $S^2_{\hat{A}}$ are the local mean and variance of neighborhood pixels in a window w_1, since there are only N states, the probabilities $\Pr\{\hat{A}(i,j) = q_n\}$ can be normalized to their sum. Based on the above definitions the final entropy is expressed as

$$-\sum_{n=1}^{N} \frac{\Pr\{\hat{A}(i,j) = q_n\}}{\xi} \log\left(\frac{\Pr\{\hat{A}(i,j) = q_n\}}{\xi}\right), \tag{4}$$

where $\xi = \sum_{n=1}^{N} \Pr\{\hat{A}(i,j) = q_n\}$. By replacing the probability definitions, (4) is expressed as

$$H_l(i,j) = \frac{1}{2} \ln(2\pi e \sigma^2_{\hat{A}}(i,j)) \tag{5}$$

Therefore, the minimum entropy region is the region that has minimum variance and is the more structured and uniform region. We improve the performance of the restoration technique by introducing a minimum entropy approach to detect this more structured region surrounding each pixel.

3.2 The proposed HMM method

The proposed method is based on finding the most likely gray level at each pixel, this is performed according to the probabilities of noisy observations of individual states. The noisy observation probability $\Pr\{S(i,j) = Q_n | Q_n\}$ is defined as the probability that the state matrix centered at pixel (i,j), i.e., $S(i,j)$ is equal to one of the N^{XY} state matrices $\{Q_n\}$ for $1 \le n \le N^{XY}$, by assuming an additive white Gaussian noise process, we have

$$\Pr\{S(i,j) = Q_n | Q_n\} = \mathcal{N}((o(i,j) - HQ_n); \sigma^2_n) \tag{6}$$

where $N(\cdot)$ denotes the Gaussian probability density function. $\mathbb{H}Q_n$ is computed by the sum of the products of the corresponding entries of matrices H and Q_n. This equation is a straightforward conclusion of (1). However, in the case of a large number of states, computing all these probabilities is computationally complex and the memory requirement is overbearing, by considering the shift property of the FIR filter, the enormous computational complexity can be reduced. By assuming the horizontal scanning of the image and using the shift structure of the FIR filter, we observe that the state matrices centered at pixels (i,j) and $(i,j-1)$ have some common elements, viz, the state matrix centered at pixel (i,j) is the horizontal shift of the state matrix centered at pixel $(i,j-1)$ with the new elements in its last column. Moreover, considering that the rows are estimated in the increasing order, the state matrix centered at pixel (i,j) is the vertical shift of the state matrix centered at pixel $(i-1,j)$, thus the only new element of the state matrix centered at pixel (i,j) is the element in the last row and last column of

matrix $S(i,j)$ which is denoted by $S_{XY}(i,j)$. We estimate this element by averaging over all N possible states q_n,

$$\hat{S}_{XY}(i,j) = \sum_{n=1}^{N} q_n \Pr\{S_{XY}(i,j) = q_n\}, \tag{7}$$

where $\Pr\{S_{XY}(i,j) = q_n\}$ denotes the probability that the element (x,y) of matrix $S(i,j)$ is equal to q_n, this probability can be expressed by using Bayes' equality as,

$$\Pr\{S_{xy}(i,j) = q_n\} = \mathscr{N}(o(i,j) - \mathbb{H}S(i,j); \sigma^2)\Pr\{q_n\}, \tag{8}$$

The other elements of the state matrix $S(i,j)$ that are common with the previous state matrices can be re-estimated recursively, e.g., the probability that the element (x,y) of the state matrix S_{XY} is equal to q_n; $\Pr\{S_{xy}(i,j) = q_n\}$ is

$$\begin{aligned} \Pr\{S_{xy}(i,j) = q_n\} &= \Pr\{S_{x(y+1)}(i,j-1) = q_n\}, \\ &\mathscr{N}(o(i,j) - S(i,j)|_{S_{xy}(i,j)=q_n}; \sigma_n^2), \Pr\{q_n\} \end{aligned} \tag{9}$$

Since the element (x,y) of the state matrix at (i,j) has been the $x(y+1)$ element of the state matrix at $(i,j-1)$, the probability $\Pr\{S_{xy}(i,j) = q_n\}$ is computed by the forward recursion from the probabilities of the state vector, $S(i,j-1)$, as shown in Eq. (9), by using this method the computational order is reduced from N^{XY} in Eq. (2) to XY, this strategy is tantamount what is used for channel equalization [5]. The other important probability in Eq. (9) is $\Pr\{q_n\}$ that expresses the probability of occurrence of the event q_n in the related position.

The probability $\Pr\{q_n\}$ in Eq. (9) is the probability of the occurring the gray level q_n for pixel $(i+x, j+y)$ and is expressed as,

$$\Pr\{q_n\} = N(q_n - m_{\hat{A}}(i+x, j+y); S^2_{\hat{A}}(i+x, j+y)), \tag{10}$$

where $m_{\hat{A}}(i+x, j+y)$ and $S^2_{\hat{A}}(i+x, j+y)$ are the local mean and variance of the neighborhood pixels in a window that its size has been obtained from the second stage.

3.3 The proposed algorithm

For more clarity, in the following we summarize the steps of the proposed algorithm,

1) Put $k = 1$
2) If $k = 1$, obtain the initial estimated image $\hat{A}$ from the blurred and noisy observed image o by the Wiener filtering.
3) Set $i = 0$, $j = 0$.
4) Put $i = i+1$, $j = j+1$, $x = 0$, $y = 0$.
5) If $i+x > I$ or $j+y > J$, stop the algorithm.
6) $1 = 1$ and compute $H_1(i,j)$ from Eq. (5).
7) Put $1 = 1+1$ and compute $H_1(i,j)$ from Eq. (5).
8) If $H_1(i,j) > H_{1-1}(i,j)$ then $w_1(i,j) = 1-1$ else go to step 7.
9) Compute local mean and variance $m_{\hat{A}}(i+x, j+y)$, $S^2_{\hat{A}}(i+x, j+y)$, in a window with size $w_1(i+x, j+y)$ around pixel $(i+x, j+y)$ in image $\hat{A}$ then compute $\Pr\{q_n\}$, for pixel $(i+x, j+y)$ from Eq. (10).
10) If $x \neq X$ or $y \neq Y$ compute $\Pr\{S_{XY}(i,j) = q_n\}$ from Eq. (9) else compute $\Pr\{S_{XY}(i,j) = q_n\}$ from Eq. (8).
11) Compute $\hat{S}_{XY}(i,j)$ from Eq. (7).
12) Put $\hat{A}(i+X, j+Y) = \hat{S}_{XY}(i,j)$.
13) Put $x = x+1$ and $y = y+1$ then go to step 4.
14) If $k < 2$, put $k = k+1$ and go to step 3 else stop the algorithm.

4. Simulation results

The proposed algorithm was compared with the regularized filter [6] and Lucy-Richardson [7]. In order to quantitatively evaluate the performance of these methods, we estimate PSNR (Peak Signal to Noise Ratio) between the restored image and the original image. Experiments were carried out on test images in the case of one and two-dimensional blurred functions.

The results show the superiority of the HMM method over the regularized filter and the Lucy-Richardson method especially when the one-dimensional blur is too extended, meanwhile, the results of the proposed algorithm in the case of two-dimensional blur are nearly the same as the other methods.

The PSNR values for different methods are shown in Table 1 in the case of motion-blurred images for the square blur extending in the range of 11 to 51 and at SNR = 25 dB. This table shows the PSNR improvement of the HMM method over the other three methods, it is also observed from the table that the PSNR values for the Wiener filter increase by increasing the blur extension, this is due to the fact that the Wiener filter maintains the details of image along with the noise effect thus at a constant SNR whatever the blur extend becomes larger the effect of blur overcomes the effect of noise and the structure of image becomes more obvious.

To observe the quality of the restored images the results of the mentioned methods are shown in Figs. 1 and 2 for

Table 1. PSNR values of different methods, SNR = 25 dB.

Blur extend	Wiener	Lucy-Richardson	Regularized	HMM
11	13.96	22.08	22.19	23.39
15	13.48	21.42	21.54	22.65
21	13.39	20.66	20.82	21.87
25	13.52	20.31	20.45	21.58
31	13.76	19.98	20.06	21.13
35	14.00	19.79	19.85	20.95
41	14.32	19.52	19.55	20.71
45	14.54	19.40	19.41	20.69
51	14.81	19.06	19.12	20.08

Figure 1. (a) Original image; (b) Motion blurred image with blur extend = 31, SNR = 30 dB; (c) Lucy-Richardson method, PSNR = 19.98; (d) regularized filter, PSNR = 20.06.

cameraman image corrupted by motion blur extend equal to 31 taps at SNR = 30 dB.

Figs. 1 (a) and 1 (b) show the original and motion-blurred cameraman images, respectively. Figs. 1 (c) and 1 (d) show the restored images by Lucy-Richardson and regularized filters with the resulted PSNRs equal to 19.98 and 20.06, respectively.

Fig. 2 (a) shows the result of the Wiener filter that is used for the initial image of the HMM method and Fig. 2 (b) shows the corresponding varying adaptive window sizes obtained from the second stage. In this figure, black and white correspond respectively to small and large window sizes, the adaptive window size delineates the contours of the image.

Fig. 2 (c) shows the restored image obtained from the first step that is used as the initial image for the third step and Fig. 2 (d) shows the corresponding window size image obtained from the second stage, in comparison with Fig. 2 (b) ,this figure exhibits the edgy structure of the image with more precise.

In Fig. 2 (e) there is the restoration result of the fourth stage that is assumed as the final result of the HMM method. This figure shows the high quality and detailed preservation of the HMM method in comparison with the other methods.

5. Conclusions

In this paper, a new method for image motion deblurring has been presented using a combination of the Wiener filter, HMM algorithm, and minimum entropy approaches. The introduced method takes full advantage of the statistical information embedded in the image. We have determined the windows that acquire minimum entropy thus least randomness and more structured shape to increase their applicability for image restoration. This minimum randomness along with the EM method can reduce the variance of the estimation noise further to provide more visibility, thus with the new strategy not only the noise is reduced considerably but also the detailed structure of the image is recovered. By these, we observe high improvement in the estimation process and image restoration over the existing methods.

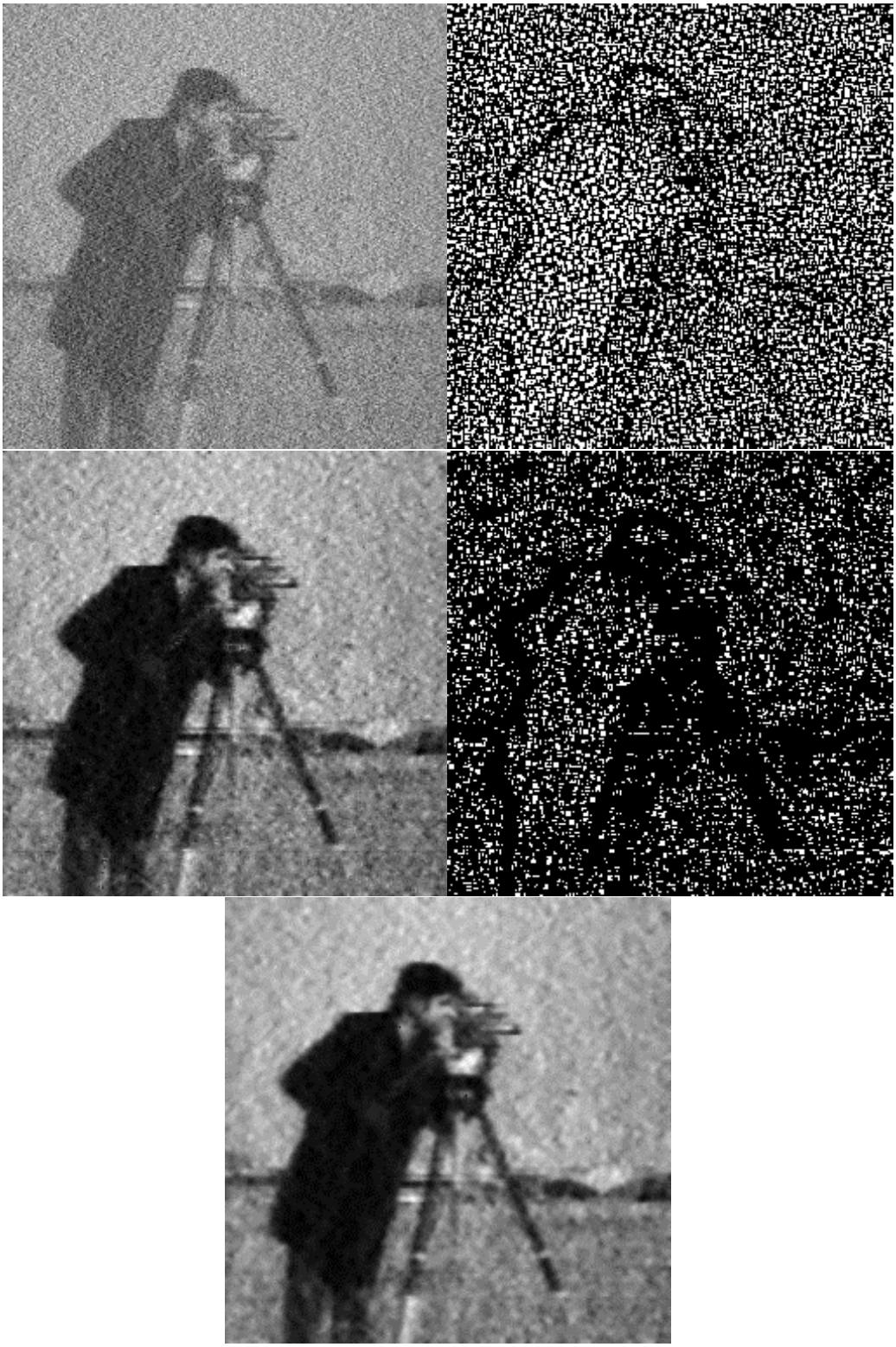

Figure 2. (a) Wiener filter, PSNR = 13.76; (b) Window size image at step 1; (c) Restored image in step 1 of HMM method, PSNR = 20.55; (d) Window size image at step 2, PSNR = 21.13; (e) Restored image in step 2 of HMM method.

Acknowledgement

We would like to acknowledge, Islamic Azad university, central Tehran branch for supporting the extra-university research project with Saman Industrial Complex, entitled "Feasibility and Conceptual Design of the Optimization of DOA and Localization Algorithms Using Artificial Intelligence Methods".

Authors contributions
Authors have contributed equally in preparing and writing the manuscript.

Availability of data and materials
The data that support the findings of this study are available from the corresponding author upon reasonable request.

Conflict of interests
The authors declare that they have no known competing financial interests or personal relationships that could have appeared to influence the work reported in this paper.

References

[1] D. Kundur and D. Hatzinakos. "Blind Image Deconvolution.". *IEEE Signal Processing Magazine*, 13(3):43–64, 1996.

[2] S. J. Reeves and R. M. Mersereau. "Blind identification by the method of generalized cross-validation.". *IEEE Trans. on Image Processing*, 1(3):301–311, 1992.

[3] A. Tikhonov. "Solution of incorrectly formulated problems and the regularization method.". *Soviet Math. Dokl.*, pages 1032–1038, 1963.

[4] V. Krishnamurthy and J. B. Moore. "On-Line Estimation of hidden Markov Model Parameters Based on the Kullback-Leibler Information Measure.". *Biomedical Engineering Letters*, 6:66–73, 2016.

[5] L. B. White, S. Perreau, and P. Duhamel. "Reduced Computation Blind Equalization for FIR channel input Markov Models.". *ICC'*, 95:673–678, 1995.

[6] R. C. Gonzalez and R. E. Woods. "Digital Image Processing.". *Addison-Wesley*, 1992.

[7] R. J. Hanisch, R. L. White, and R.L. Gilliland. "Deconvolution of Images and Spectra.". *Academic Press*, 1997.

[8] Zh. Xinzhong et al. "Noisy Motion-blurred Images Restoration Based on RBFN.". *J. Res. Pract. Inf. Technol.*, 41:195–222, 2009.

[9] L. Chen, X. Tian, S. Xiong, Y. Lei, and C. Ren. "Unsupervised Blind Image Deblurring Based on Self-Enhancement.". *IEEE/CVF Conference on Computer Vision and Pattern Recognition (CVPR)*, pages 25691–25700, 2024.

[10] W. Chu, Z. Cheng, and L. He. "Semi-Supervised Atmospheric Turbulence Mitigation Based on Hybrid Models.". *IEEE Access*, 12: 174527–174538, 2024.

[11] Z. Yue, H. Yong, Q. Zhao, L. Zhang, D. Meng, , and K. Y. K. Wong. "Deep Variational Network Toward Blind Image Restoration.". *IEEE Transactions on Pattern Analysis and Machine Intelligence*, 46(11): 7011–7026, 2024.